11416–11427 *Nucleic Acids Research, 2012, Vol. 40, No. 22* *Published online 9 October 2012*
doi:10.1093/nar/gks920

Mek1 stabilizes Hop1-Thr318 phosphorylation to promote interhomolog recombination and checkpoint responses during yeast meiosis

Chi-Ning Chuang[1,2], Yun-Hsin Cheng[1,2] and Ting-Fang Wang[1,2,*]

[1]Institute of Molecular Biology, Academia Sinica, Taipei 115 and [2]Institute of Genome Sciences, National Yang-Ming University, Taipei 112, Taiwan

Received April 11, 2012; Revised September 8, 2012; Accepted September 11, 2012

ABSTRACT

Red1, Hop1 and Mek1 are three yeast meiosis-specific chromosomal proteins that uphold the interhomolog (IH) bias of meiotic recombination. Mek1 is also an effector protein kinase in a checkpoint that responds to aberrant DNA and/or axis structure. The activation of Mek1 requires Red1-dependent Hop1-Thr(T)318 phosphorylation, which is mediated by Mec1 and Tel1, the yeast homologs of the mammalian DNA damage sensor kinases ATR and ATM. As the ectopic expression of Mek1-glutathione *S*-transferase (GST) was shown to promote IH recombination in the absence of Mec1/Tel1-dependent checkpoint function, it was proposed that Mek1 might play dual roles during meiosis by directly phosphorylating targets that are involved in the recombination checkpoint. Here, we report that Mek1 has a positive feedback activity in the stabilization of Mec1/Tel1-mediated Hop1-T318 phosphorylation against the dephosphorylation mediated by protein phosphatase 4. Our results also reveal that GST-Mek1 or Mek1-GST further increases Hop1-T318 phosphorylation. This positive feedback function of Mek1 is independent of Mek1's kinase activity, but dependent on Mek1's forkhead-associated (FHA) domain and its arginine 51 residue. Arginine 51 directly mediates the interaction of Mek1-FHA and phosphorylated Hop1-T318. We suggest that the Hop1–Mek1 interaction is similar to the Rad53-Dun1 signaling pathway, which is mediated through the interaction of phosphorylated Rad53 and Dun1-FHA.

INTRODUCTION

In most sexually reproducing organisms, programmed DNA double-strand breaks (DSBs) are necessary for generating crossovers (COs) between homologous chromosomes to ensure accurate segregation during the first meiotic division (1). In contrast, the recombination-mediated repair of DSBs uses the sister templates during mitosis (2). Thus, a unique aspect of meiotic recombination is the choice between three recombination templates (two homologs and one sister chromatid) to repair a DSB. In *Saccharomyces cerevisiae*, the formation of DSBs requires the evolutionarily conserved transesterase Spo11 and several accessory factors (1). These DSBs are resected by the Mre11–Rad50–Xrs2 (MRX) nuclease complex, Sae2 and Exo1 nuclease ensemble to generate 3′-single-strand DNA (ssDNA) tails that invade the intact DNA duplexes used in DNA repair (3–5). Overhangs of 3′-ssDNA are initially bound by replication protein A (RPA) and then replaced by RecA-like strand exchange proteins, Rad51 and Dmc1 (6). The resulting nucleoprotein filaments mediate the search for homology and catalyze DNA strand exchange to form joint molecule intermediates. Dmc1 and Rad51 have overlapping but also non-redundant functions in promoting recombination during meiosis (7). Eventually, the DSBs are repaired, resulting in COs, with the exchange of chromosome arms or non-COs (NCOs). Three meiosis-specific proteins, Mek1, Hop1 and Red1, act positively to promote interhomolog (IH) recombination (8–10) and negatively to slow the rate of intersister recombination (11). The faster rate of intersister repair is mediated by sister chromatin cohesion (Rec8), while Red1/Hop1/Mek1 counteracts this effect, thereby ensuring IH bias (12).

Mek1 is a protein kinase, whereas Red1 and Hop1 are structural components of the axial elements of the

*To whom correspondence should be addressed. Tel: +886 2 27899188; Fax: +886 2 27826508; Email: tfwang@gate.sinica.edu.tw

synaptonemal complex (SC). The SC is a zipper-like proteinaceous structure that mediates chromosome synapsis during the late prophase stage known as pachytene. The SC consists of a central region and two dense lateral elements. The lateral element constitutes the rod-like homolog axis, which is called an axial element prior to synapsis (13–17). The central region of the SC is made up of Zip1 (18). In response to DSBs, Red1 associates with SUMO polymeric chains (19) and the 9-1-1 complex (Ddc1–Mec3–Rad17) (20) to activate Mec1 and Tel1, the yeast homologs of the mammalian DNA damage sensor kinases ATM and ATR. These two kinases preferentially phosphorylate their substrates at serine (S) and threonine (T) residues that precede glutamine residues, so-called SQ/TQ motifs. Many known targets of the ATM/ATR family proteins contain the SQ/TQ cluster domains (SCDs). For example, Mec1 and Tel1 phosphorylate Hop1 at multiple SQ/TQ motifs within its N-terminal SCD (amino acid residues 298–319), in which the phosphorylation of T318 affects Hop1 activities most profoundly (21). Hop1-T318 phosphorylation is required for the activation of Mek1 and its recruitment to chromosomes (21), consistent with previous reports that Mek1 activation requires both Red1 and Hop1 (8,9). Mec1 and Tel1 also phosphorylate SQ and TQ sites in several other phosphoproteins during meiosis, including Sae2, histone H2A at S129 (i.e. γ-H2A), RPA, Rad53 and Zip1 (22–26). The Mec1-dependent phosphorylation of the Zip1 protein at S75 dynamically destabilizes homology-independent centromere pairing in response to DSBs (26). Protein phosphatase 4 (PP4) is responsible for the dephosphorylation of several Mec1/Tel1-dependent phosphoproteins during meiosis, as persistent hyperphosphorylation occurs in the absence of Pph3 and Psy2 (26). Pph3 and Psy2 are the catalytic subunit and the coactivator of PP4, respectively (27,28). Finally, the presence of aberrant DNA structures or incomplete synapsis activates a Mec1/Tel1-dependent recombination checkpoint that leads to the inhibition of Ndt80, a transcription factor required for the exit from pachytene (29,30).

Mek1 phosphorylates multiple targets in meiosis, including Rad54 at T132 (31), and histone H3 at T11 (32). Rad54 is a dsDNA-dependent ATPase that is required for Rad51 recombinase activity (33). The *mek1Δ* mutant generates very few viable spores. However, a *rad54*^{T132A} allele that substitutes T132 with alanine (A) displayed no apparent defect in spore viability. Phosphorylated Rad54 might act synergistically with the meiosis-specific protein Hed1 to suppress the recombinase activity of Rad51 (31). Alternatively, Rad54 phosphorylation may have little effect on preventing intersister recombination or another protein Tid1/Rdh54 can substitute Rad54 and use Dmc1 for IH recombination (34,35). The role of H3-T11 phosphorylation is still unclear. It was also suggested that Mek1 might directly phosphorylate targets that are involved in establishing IH bias (10). Mek1 activation can be artificially maintained through glutathione *S*-transferase (GST)-mediated dimerization. Mek1-GST and GST-Mek1 can rescue the spore viability of *mek1Δ* but not *hop1Δ* or *red1Δ* (8,36). Intriguingly, the ectopic expression of Mek1-GST in wild-type cells results in increased IH bias, but the extraneous IH events are preferentially repaired as NCOs rather than COs. In contrast, Mek1-GST promotes both IH bias and CO formation in the absence of *RAD17*- and *PCH2*-dependent checkpoint functions (36). Rad17 is a component of the 9-1-1 checkpoint complex (20). Pch2 is a widely conserved, putative ATPase associated with cellular activities (AAA)-type ATPase with important roles in pachytene checkpoint, normal SC assembly, and the distribution of DSBs and CO events (37–48). Recently, Pch2 was shown to physically and functionally interact with Xrs2 (49) and Tel1 (Wang,T.-F., unpublished data). Xrs2 is a member of the MRX complex, which acts at the sites of unprocessed DSBs. It has been suggested that the Pch2–Xrs2 interaction might enable Pch2 to remodel chromosome structures adjacent to DSB sites to promote access by Tel1 and Mec1 kinases for Hop1 phosphorylation (49). As Mek1-GST is involved in promoting IH bias in the absence of *RAD17*- and *PCH2*-dependent checkpoint functions, Mek1 was proposed to phosphorylate proteins that are directly involved in the recombination checkpoint (36). In this report, we further explored the roles of Mek1, GST-Mek1 and Mek1-GST in regulating the recombination checkpoint. Our data support an alternative model in which Mek1 provides positive feedback in the stabilization of Mec1/Tel1-mediated Hop1-T318 phosphorylation.

MATERIALS AND METHODS

Antisera

Guinea pig antisera against phosphorylated Zip1-S75 were raised using a synthetic phosphopeptide (C^{65}KKLITSMSLS$^{[P]}$QRNHGYS^{82}) as an antigen. Rabbit antisera against phosphorylated Rad54-T132 and phosphorylated Hop1-T318 were raised using the synthetic phosphopeptides (T^{126}LRRSFT$^{[P]}$VPIKGYV^{139} and S^{311}QASIQPT$^{[P]}$QFVSNN^{324}) as antigens, respectively. The antisera were pre-cleared by affinity chromatography using the corresponding non-phosphorylated peptides coupled to agarose beads. Phosphopeptide synthesis and animal immunization were conducted by LTK BioLaboratories, Taiwan. Anti-phospho-Histone 2A (H2A)-S129 antiserum (50) was from Millipore, Billerica, MA, USA. Anti-GST antibody was from Genescript, NJ, USA. Anti-YFP (or anti-GFP) antibody was from Clontech, CA, USA.

Yeast strains, sporulation and western blot analysis

All meiotic experiments were performed using diploid cells from the SK1 strain background. Western blot analyses were performed as previously described (19,51). Spore viability was determined by tetrad dissection.

Inhibition of the analog-sensitive GST-Mek1-as mutant

4-Amino-1-tert-butyl-3(1′-naphthylmethyl)pyrazolo[3,4-*d*]pyrimidine (1-NM-PP1) (52) was provided by Cellular Genomics (New Haven, CT, USA). Five micromolars of

1-NM-PP1 was added into sporulating cell culture to inhibit GST-Mek1-as kinase activity.

Quantitative western blot analyses

Yeast total protein extracts were prepared by trichloroacetic acid precipitation as previously described (51). Western blots were developed using the ChemiLucent ECL Detection System (Millipore) and imaged by exposure to X-ray film. The relative intensities of protein bands of interest from X-ray films were obtained with a Biospectrum 600 imaging system (UVP, Upland, CA, USA) containing an OptiCam 600 camera (Canon, Japan). For quantification, protein bands were plotted on a bar graph using VisionWorksLS Image Acquisition and Analysis Software (UVP). The intensities of phosphorylated Hop1-T318 proteins (72–95 kDa) and of the loading control (Hsp104) were acquired from X-ray films by subtracting an equally sized background, respectively. For normalization, intensity of phosphorylated Hop1-T318 protein was divided by that of the loading control at the indicated time point. To reduce the quantitative variations resulting from different X-ray film exposure time, the protein samples with the strongest phosphorylated Hop1-T318 signals were collected from different cultures and simultaneously compared in a separate western blot.

RESULTS

Validation of antisera against phosphorylated Hop1-T318, Zip1-S75 and Rad54-T132 proteins

Phosphorylated peptides were synthesized and used to generate antisera specific to phosphorylated Hop1-T318, Zip1-S75 and Rad54-T132 proteins (see 'Materials and Methods' section). Synchronous meiosis was induced in wild-type and mutant strains. Following transfer to sporulation medium, meiotic cells were harvested at the indicated time points, and total cell lysates were prepared (51). Western blot analyses were performed to validate these antisera. As shown in Figure 1A (middle panel), at least two bands (~85 kDa) were detected by anti-phospho-Hop1-T318 antibodies in the wild-type lysate, but not in the lysates from strains carrying mutant alleles *hop1Δ* or $hop1^{T318A}$ *dmc1Δ*. The $hop1^{T318A}$ variant encodes a mutant protein in which the T318 residue of Hop1 has been mutated to alanine (A); this strain produces no viable spores (Table 1) (21). The *dmc1Δ* mutation results in the accumulation of resected DSBs (or ssDNAs) (53) and phosphorylated Hop1 (21). T318 is not the sole phosphorylation site in Hop1 (21), as shifted bands are still detected by anti-Hop1 antisera in wild type and $hop1^{T318A}$ *dmc1Δ* (Figure 1A). Next, we showed that the extent of Hop1-T318 phosphorylation is comparable between wild type and *tel1Δ* but reduced in *mec1-kd* (=kinase dead) *sml1Δ* (Figure 1B; *sml1Δ* suppresses the lethality conferred by *mec1Δ* or *mec1-kd* mutations). Phosphorylated Hop1-T318 is not detected with anti-phospho-Hop1-T318 antisera in the *mec1-kd sml1Δ tel1Δ* triple mutant. Furthermore, shifted Hop1 band is hardly recognized by anti-Hop1 antisera in the *mec1-kd sml1Δ tel1Δ* triple mutant (Figure 1B).

The dephosphorylation of Hop1-T318 is mediated by PP4 in meiosis, and the persistent hyperphosphorylation of Hop1-T318 was observed in *pph3Δ* (Figure 1C). Pph3 is the catalytic subunit of PP4. The *pph3Δ* mutant also accumulated higher levels of phosphorylated Zip1; shifted bands were detected with anti-Zip1 antibody (Figure 1C). The anti-phospho-Zip1-S75 antibodies were able to detect phosphorylated Zip1-S75 in the wild type but not in the *zip1Δ* or the *mec1-kd sml1Δ tel1Δ* triple mutant (Figure 1D). These results confirmed that Mec1 and Tel1 mediate Hop1 and Zip1 phosphorylation (21,26) and that PP4 is responsible for Hop1 and Zip1 dephosphorylation (26). Finally, the anti-phospho-Rad54-T132 antibody specifically recognizes phosphorylated Rad54-T132, as suggested by the absolute dependence of a positive signal in western blotting on the phosphorylation of T132. This band is absent in a strain carrying the $rad54^{T132A}$ mutation despite normal entry into meiosis, as indicated by timely appearance of SC protein Zip1 (Figure 1E).

Mek1 promotes not only Rad54-T132 phosphorylation but also Hop1-T318 phosphorylation

Mek1 mediates Rad54-T132 phosphorylation during meiosis (31). Phosphorylated Rad54-T132 was detected with anti-phospho-Rad54-T132 antisera in *mek1Δ* diploids transformed with either a P_{MEK1}-*MEK1* or P_{MEK1}-*GST-mek1-as* expression vector, in which the expression of Mek1 or GST-Mek1-as, respectively, is under the control of the *MEK1* gene promoter (P_{MEK1}). *GST-mek1-as*, an analog-sensitive mutant, has the advantage that it can be specifically inhibited by the addition of the purine analog 1-NM-PP1, whereas wild-type GST-Mek1 is unaffected by inhibitor (9,31). Quantitative western blot analyses (see 'Materials and Methods' section) showed that Rad54-T132 phosphorylation was negligible in a *mek1Δ* strain carrying a mock 2 μ vector. Higher steady-state levels of phosphorylated Rad54-T132 were induced by GST-Mek1-as (in the absence of 1-NM-PP1) than by Mek1 in *mek1Δ* (Figure 2A and B). Thus, in accordance with the semi-dominance of GST-Mek1 and Mek1-GST, semi-dominance can also be assumed for GST-mek1-as (8,36).

Mek1 is a downstream effector of phosphorylated Hop1-T318 (21). Surprisingly, we observed that Mek1 and GST-Mek1-as enhanced Hop1-T318 phosphorylation but not Zip1-S75 phosphorylation or H2A-S129 phosphorylation in *mek1Δ*. Overexpression of GST-Mek1-as in *mek1Δ* induced persistent and higher steady-state levels of Hop1-T318 phosphorylation, whereas overexpression of Mek1 in *mek1Δ* induced a transient increase of Hop1-T318 phosphorylation (Figure 2A and B). In contrast, the steady-state levels of Zip1-S75 phosphorylation and H2A-S129 phosphorylation were slightly lower in P_{MEK1}-*GST-mek1-as mek1Δ* than in P_{MEK1}-*MEK1 mek1Δ* or in *mek1Δ* (Figure 2A and B). As all these three phosphoproteins are mediated by the Mec1 and Tel1 kinases, it is unlikely that the positive

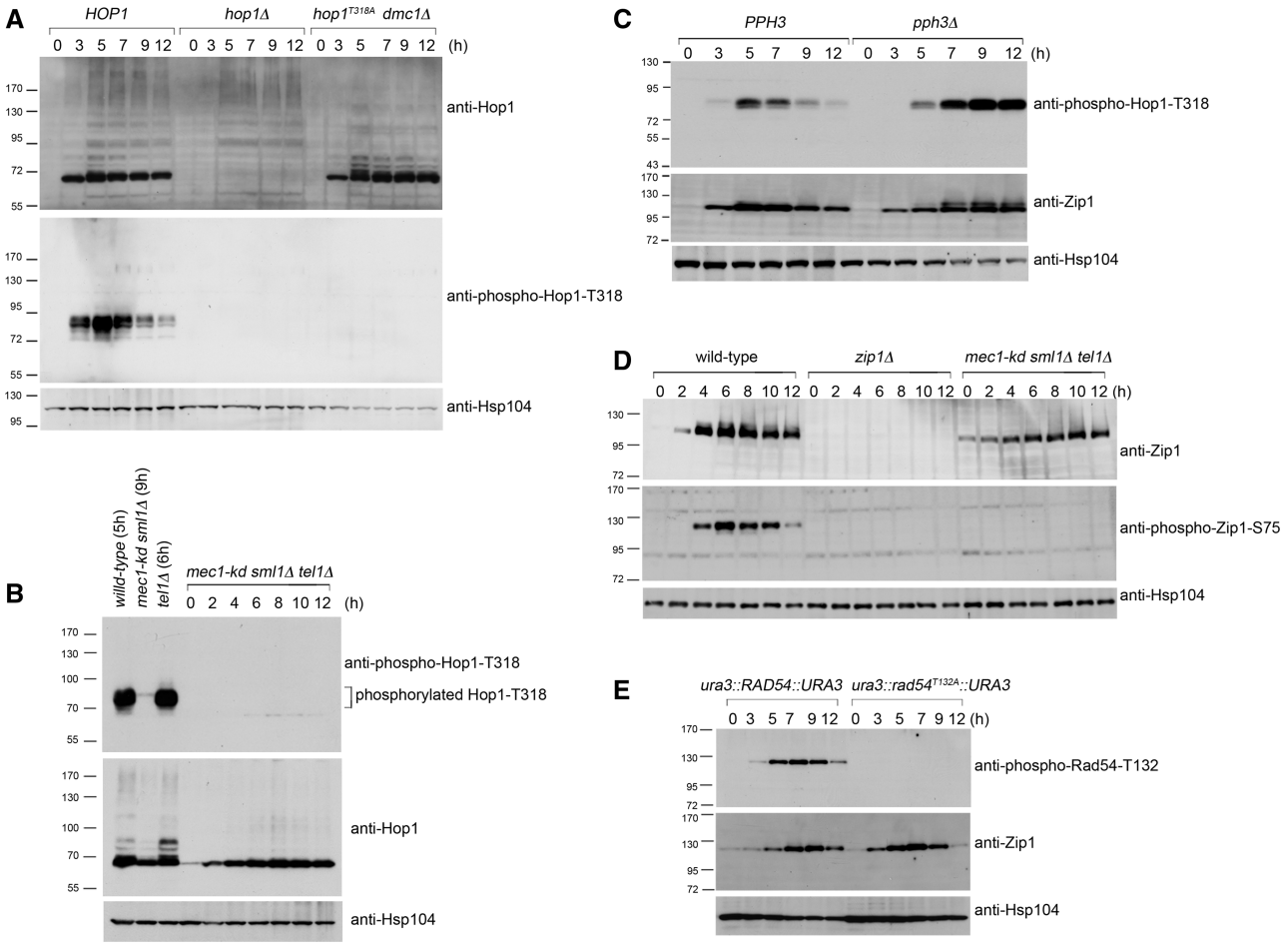

Figure 1. Validation of antisera against phosphorylated Hop1-T318 (**A–C**), Zip1-S75 (**D**) and Rad54-T132 (**E**). Western blot time course analyses of meiotic cells were performed as described previously (19,51). Wild-type and mutant strains at different sporulation time points are indicated. Anti-Hop1, anti-Zip1, anti-phospho-Hop1-T318, anti-phospho-Rad54-T132 and anti-phospho-Zip1-S75 antibodies were used to detect the corresponding proteins. Antibody against Hsp104 was used as a loading control. Molecular weights (in kiloDaltons) are indicated to the left of the blots.

feedback function of GST-Mek1-as or Mek1 on Hop1-T318 phosphorylation is due to increased Mec1 and Tel1 kinase activities.

Since we were unable to generate or acquire antisera that could specifically recognize both phosphorylated and non-phosphorylated Rad54 in yeast total cell lysates, we next constructed yeast strains expressing yellow fluorescent protein (YFP) tagged Rad54 proteins (i.e. Rad54-YFP) (54) to determine whether *mek1Δ* mutation would affect steady-state levels of Rad54 as detected by an anti-YFP antibody (Figure 2E). Similar to the wild-type strain, the *RAD54-YFP* strain generates 89% viable spores. The *mek1Δ RAD54-YFP* mutant produces 4% viable spores (Table 1). The results of quantitative western blot analyses confirm that these two strains display similar levels of Rad54-YFP proteins during meiosis (Figure 2E and F).

GST-mediated Mek1 dimerization resulted in enhanced Hop1-T318 phosphorylation

GST-Mek1-as is better than Mek1 in enhancing Hop1-T318 and Rad54-T132 phosphorylation. GST artificially enhances dimerization of wild-type Mek1, although the role of dimerization in promoting Hop1-T318 phosphorylation is not yet clear. This possibility that GST-enhanced dimerization was responsible for the increased phosphorylation of Hop1-T318 and Rad54-T132 was addressed by constructing a non-dimerizing *gst(nd)-mek1-as* allele (8). The gst*(nd)-mek1-as* strain, similar to *GST-mek1-as* (Table 1), *mek1-GST* and *mek1-gst(nd)* (36), produces a large number of viable spores. Quantitative western blot analyses revealed that GST-Mek1-as appeared ~1 h earlier than GST(nd)-Mek1-as. Moreover, the expression levels of GST-Mek1-as were greater than those of GST(nd)-Mek1-as. We also observed that the G*ST-mek1-as* strain resulted in higher levels of Hop1-T318 phosphorylation and Rad54-T132 phosphorylation compared with the *gst(nd)-mek1-as* strain (Figure 2C and D). As the relative ratios of phosphorylated Rad54-T132 or phosphorylated Hop1-T318 versus GST-Mek1-as were similar to those of phosphorylated Rad54-T132 or phosphorylated Hop1-T318 versus GST(nd)-Mek1-as, we inferred that GST-mediated dimerization was unlikely directly responsible for the enhancement of Hop1-T318 and Rad54-T132

Table 1. Genotypes and spore viability[a]

Strain	Genotype	% Viable spores	Numbers of spores
WHY3285	*ho::hisG/″, leu2::hisG/″, HIS4::LEU2*-(BamHI)/*his4-X::LEU2*-(BamHI)–*URA3*	98	204
WHY2947	*hop1Δ/″*	0	144
WHY8853[b]	*hop1Δ/″, ura3::hop1^{T318A}::URA3/″, dmc1Δ/″*	n.d.[c]	n.d.
WHY7706	*tel1Δ/″*	85	240
WHY9047[b]	*mec1-kd/″, sml1Δ/″*	28	216
WHY9754	*mec1-kd/″, sml1Δ/″, tel1Δ/″*	0	216
WHY9174	*pph3Δ/″*	n.d.	n.d.
WHY10228	*mek1Δ/″, P_{MEK1}-mek1-as-V5* (2 μ)	96	216
WHY9384	*mek1Δ/″*, mock vector (2 μ)	3	212
WHY9978	*mek1Δ/″, P_{MEK1}-MEK1* (2 μ)	94	208
WHY9385	*mek1Δ/″, P_{MEK1}-GST-mek1-as* (2 μ)	95	212
WHY10134	*mek1Δ/″, P_{MEK1}-GST-mek1^{R51A}-as* (2 μ)	4	212
WHY9386	*hop1Δ/″, ura3::hop1^{T318A}::URA3/″*, mock vector (2 μ)	<1	108
WHY9387	*hop1Δ/″, ura3::hop1^{T318A}::URA3/″, P_{MEK1}-GST-mek1-as* (2 μ)	<1	96
WHY9755[d]	*rad54Δ/″, ura3:: RAD54::URA3/″*	90	212
WHY9746[d]	*rad54Δ/″, ura3:: rad54^{T132A}::URA3/″*	92	212
WHY2766	*rad51Δ/″, dmc1Δ/″*	n.d.	n.d.
WHY9954	*rad51Δ/″, dmc1Δ/″, mek1Δ/″*	n.d.	n.d.
WHY9083	*pch2Δ/″*,	99	144
WHY9382[e]	*pch2Δ/″, rad17Δ/″, MEK1-GST/″*	52	144
WHY9383[e]	*pch2Δ/″, rad17Δ/″*	<1	128
WHY10175	*mek1Δ/″, P_{MEK1}-gst(nd)-mek1-as* (2 μ)	80	216
WHY10281	*RAD54-YFP/RAD54-YFP*	89	216
WHY10315	*RAD54-YFP/RAD54-YFP, mek1Δ/″*	4	208

[a]All strains are SK1 *MAT***a**/*MAT*α diploids. Tetrads with four spores were dissected and analyzed following sporulation in liquid medium at 30°C.
[b]WHY8853 and WHY9047 were gifts from Rita Cha (21).
[c]n.d. (not determined).
[d]WHY9755 and WHY9746 were gifts from Nancy Hollingsworth (31).
[e]WHY9382 and WHY9383 were gifts from Sean Burgess (36).

phosphorylation. Rather, GST-Mek1-as is apparently more stable than GST(nd)-Mek1-as.

The protein kinase activity of Mek1 is not required for enhanced Hop1-T318 phosphorylation

Next, we confirmed that the protein kinase activities of GST-Mek1-as and Mek1-as are not required for the enhancement of Hop1-T318 phosphorylation. To monitor the Mek1-as protein levels, the *mek1Δ* mutant was transformed with a *P_{MEK1}-mek1-as-V5* expression vector. The *mek1-as-V5* allele encodes a V5-tagged Mek1-as protein. An addition of 5 μM 1-NM-PP1 to *mek1Δ P_{MEK1}-GST-mek1-as* (Figure 3A and B) and *mek1Δ P_{MEK1}-mek1-as-V5* (Figure 3C and D) meiotic cells greatly diminished Rad54-T132 phosphorylation (31). In contrast, Hop1-T318 phosphorylation in *mek1Δ P_{MEK1}-GST-mek1-as* (Figure 3A and B) and *mek1Δ P_{MEK1}-mek1-as-V5* (Figure 3C and D) was not affected or was only slightly affected by 1-NM-PP1, respectively. Thus, GST-Mek1-as and Mek1-as may not phosphorylate proteins that are directly involved in the Mec1/Tel1 recombination checkpoint.

Mek1 promotes Hop1-T318 phosphorylation in the presence of unrepaired DSBs

DSBs are more rapidly repaired through intersister recombination in the absence of Mek1 kinase activity (11). Mec1/Tel1-mediated Hop1 phosphorylation is DSB dependent (8,21). Accordingly, the lower Hop1-T318 phosphorylation levels detected in *mek1Δ* might simply be a consequence of faster DSB repair. This hypothesis was further examined here by comparing Hop1 and Hop1-T318 phosphorylation in *rad51Δ dmc1Δ* and *mek1Δ rad51Δ dmc1Δ*. The *rad51Δ dmc1Δ* double mutant persistently accumulates resected DSBs (or ssDNA) and produces markedly fewer CO products than the *rad51Δ* or *dmc1Δ* single mutants (53). Contrary to the hypothesis, we observed that the persistent hyperphosphorylation of Hop1-T318 and Hop1 was more profound in the *rad51Δ dmc1Δ* double mutant than in the *mek1Δ rad51Δ dmc1Δ* triple mutant (Figure 4A and B). This demonstrates that the loss of Hop1-T318 phosphorylation in the absence of Mek1 is not due to precocious DSB repair.

To further explore the effect of Mek1 on the overall Mec1 and Tel1 kinase activities in *rad51Δ dmc1Δ*, we examined Zip1-S75 phosphorylation and H2A-S129 phosphorylation by quantitative western blot analyses with anti-phospho-Zip1-S75 and anti-phospho-H2A-S129 antisera. Zip1-S75 phosphorylation was higher in *mek1Δ rad51Δ dmc1Δ* and lower in the wild-type strain than in *rad51Δ dmc1Δ* (Figure 4A and C). In contrast, similar levels of H2A-S129 phosphorylation were detected in these three strains (Figure 4A and D). The *mek1Δ* mutation is known to alleviate the prophase arrest or delay conferred by *dmc1Δ* and/or *rad51Δ* mutation (55). We found that the *mek1Δ dmc1Δ rad51Δ* triple mutant completed the first meiotic nuclear divisions (MI) faster than the *dmc1Δ rad51Δ* double mutant (Figure 4E). Thus, because the steady-state levels of Zip1 proteins were lower in the *mek1Δ dmc1Δ rad51Δ* triple mutant than in wild type or the *dmc1Δ rad51Δ* double mutant (Figure 4A, third bottom panel), we inferred that Zip1 proteins

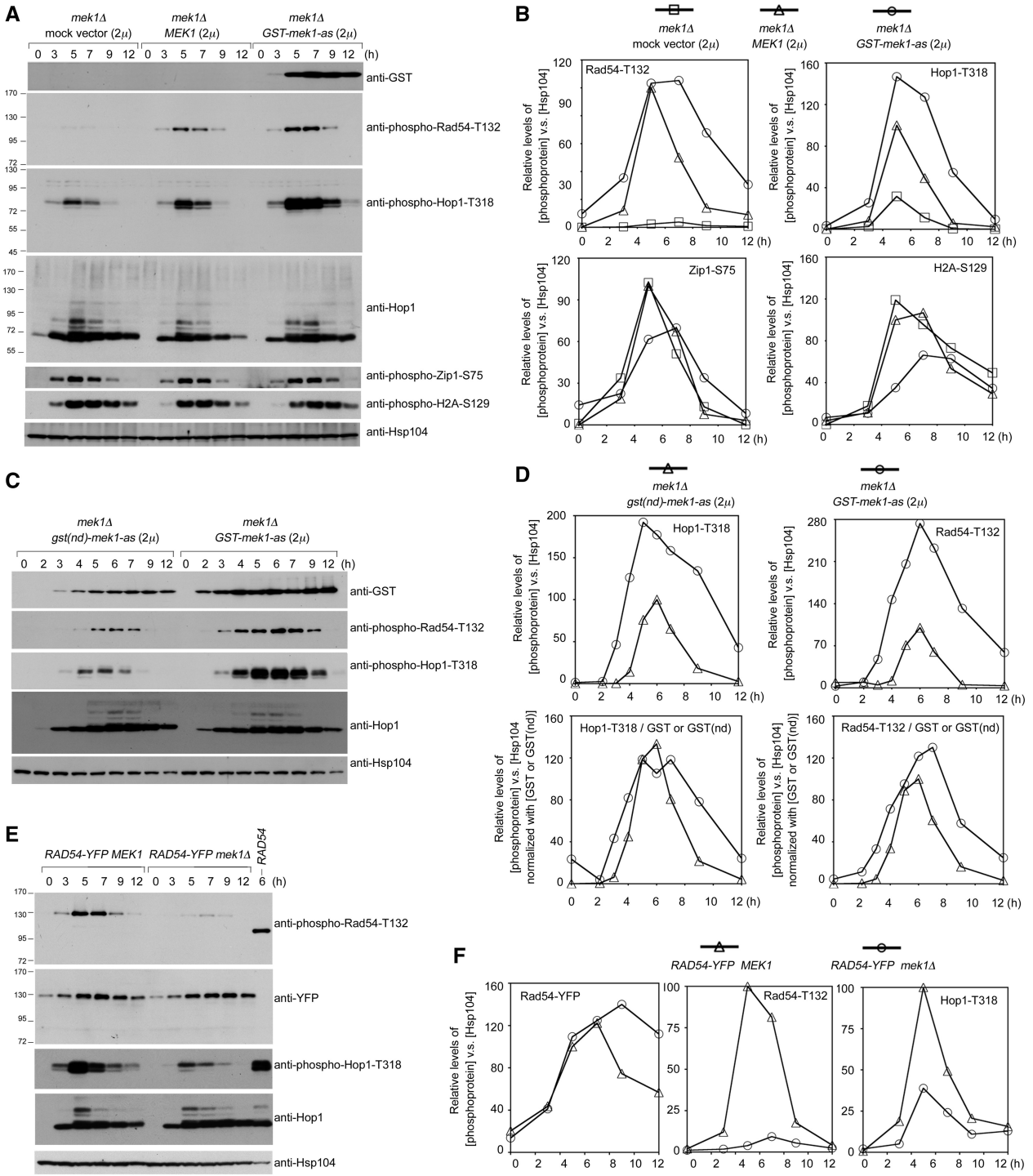

Figure 2. Mek1 and GST-Mek1-as enhance Rad54-T132 phosphorylation and Hop1-T318 phosphorylation. The *mek1Δ* diploid cells were transformed with an empty 2μ vector or a vector carrying *MEK1* (**A**), *GST-mek1-as* (A and **C**) or *gst(nd)-mek1-as* (C). The *MEK1* and *mek1Δ* diploid cells express Rad54-YFP proteins (**E**). The expression levels of various phosphoproteins were visualized by western blot analysis. (**B**, **D** and **F**) Quantitation of western blot results in (A, C and E) (see 'Materials and Methods' section). The relative levels of different phosphoproteins versus Hsp104 (loading control) at each time point are shown.

might be degraded faster in the *mek1Δ dmc1Δ rad51Δ* triple mutant. These results indicate that Mek1 does not affect overall Mec1 and Tel1 kinase activities. Mek1 might use a novel mechanism to stabilize Mec1/Tel1-mediated Hop1-T318 phosphorylation.

Hop1-T318 phosphorylation has a critical role in enhancing Mek1-mediated Hop1 phosphorylation

Hop1-T318 phosphorylation is required for both the activation and the chromosomal recruitment of Mek1 (21). To determine whether Hop1-T318 phosphorylation is also a

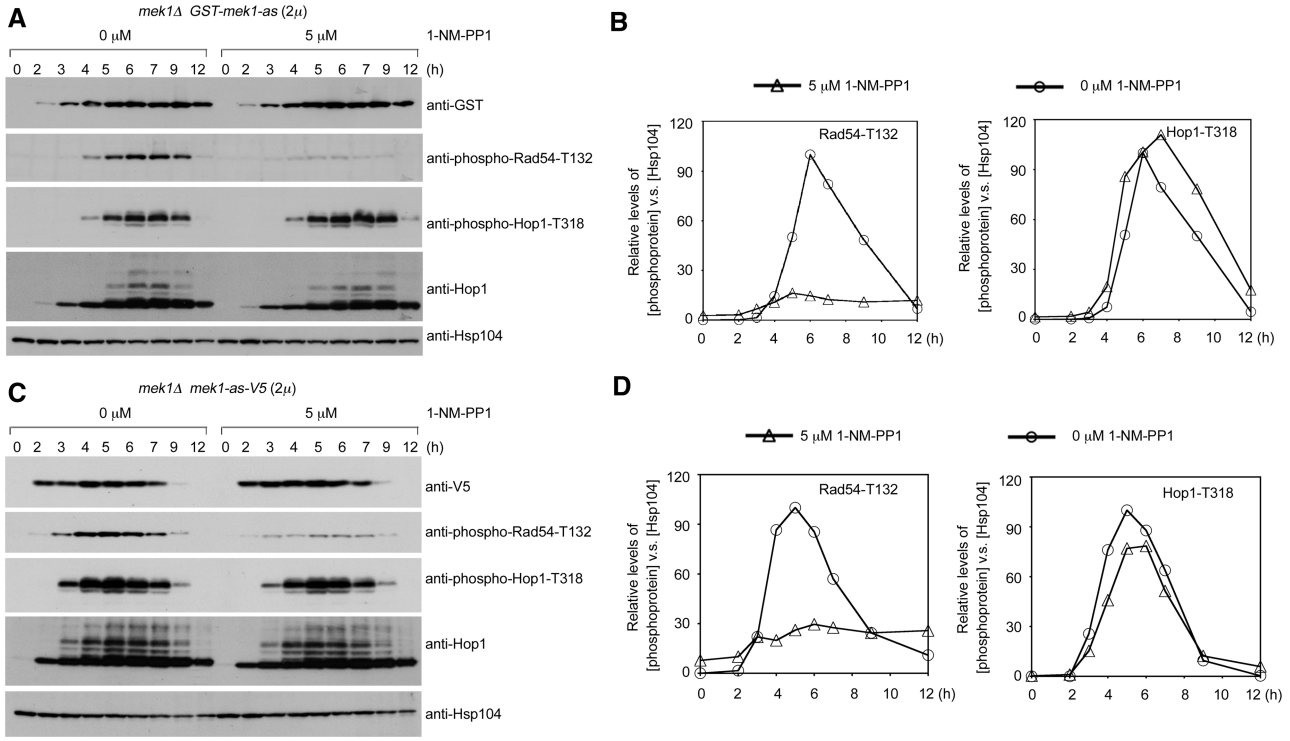

Figure 3. Mek1 kinase activity is not required for the enhancement of Hop1-T318 phosphorylation. The *mek1Δ GST-mek1-as* (2 μ) (**A**) and *mek1Δ mek1-as-V5* (2 μ) (**C**) diploid cells underwent sporulation in SPM with 0 or 5 μM 1-NM-PP1. The expression levels of various phosphoproteins were visualized by western blot analysis. (**B**, **D**) Quantitation of western blot results in (A) and (C).

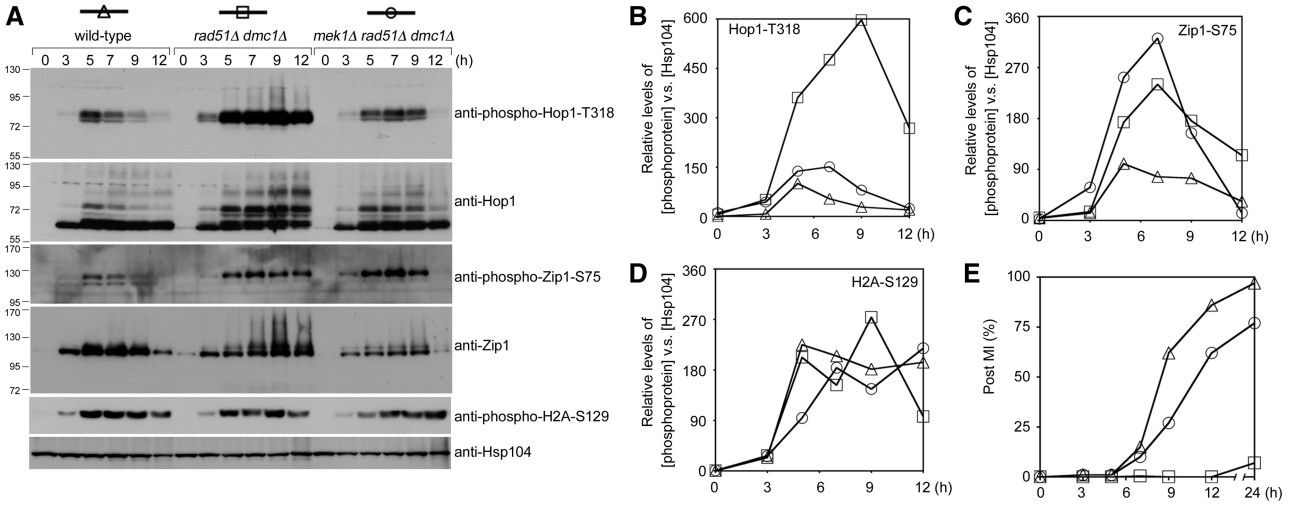

Figure 4. Mek1 promotes Hop1-T318 phosphorylation in the presence of unrepaired DSBs. (**A–D**) Quantitative western blot results of various phosphoproteins in *rad51Δ dmc1Δ* and *rad51Δ dmc1Δ mek1Δ* diploid cells. (**E**) Timing of nuclear division (MI). Cells that had completed MI were identified by determining the number of cells with two to four DAPI-staining nuclei.

prerequisite for the positive feedback function of Mek1, *GST-mek1-as* (2 μ) was introduced into the $hop1^{T318A}$ strain. In $hop1^{T318A}$, the GST-Mek1-as protein failed to rescue the levels of phosphorylated Rad54-T132 (Figure 5A) or spore viability (Table 1). No phosphorylated Hop1-T318 was detected in either strain (Figure 5A). GST-Mek1-as did not increase overall 'non-T318' Hop1 phosphorylation or H2A-S129 phosphorylation, as indicated by similar band shifts in $hop1^{T318A}$ strains carrying *GST-mek1-as* (2 μ) or a mock vector. Although GST-Mek1-as increased Zip1-S75 phosphorylation ~1.2-fold, the relative ratios of phosphorylated Zip1-S75 versus total Zip1 were similar in the presence or absence of GST-Mek1-as (Figure 5C). These results indicate that GST-Mek1-as unlikely affects overall Mec1 and Tel1 kinase activities and that Hop1-T318 phosphorylation is

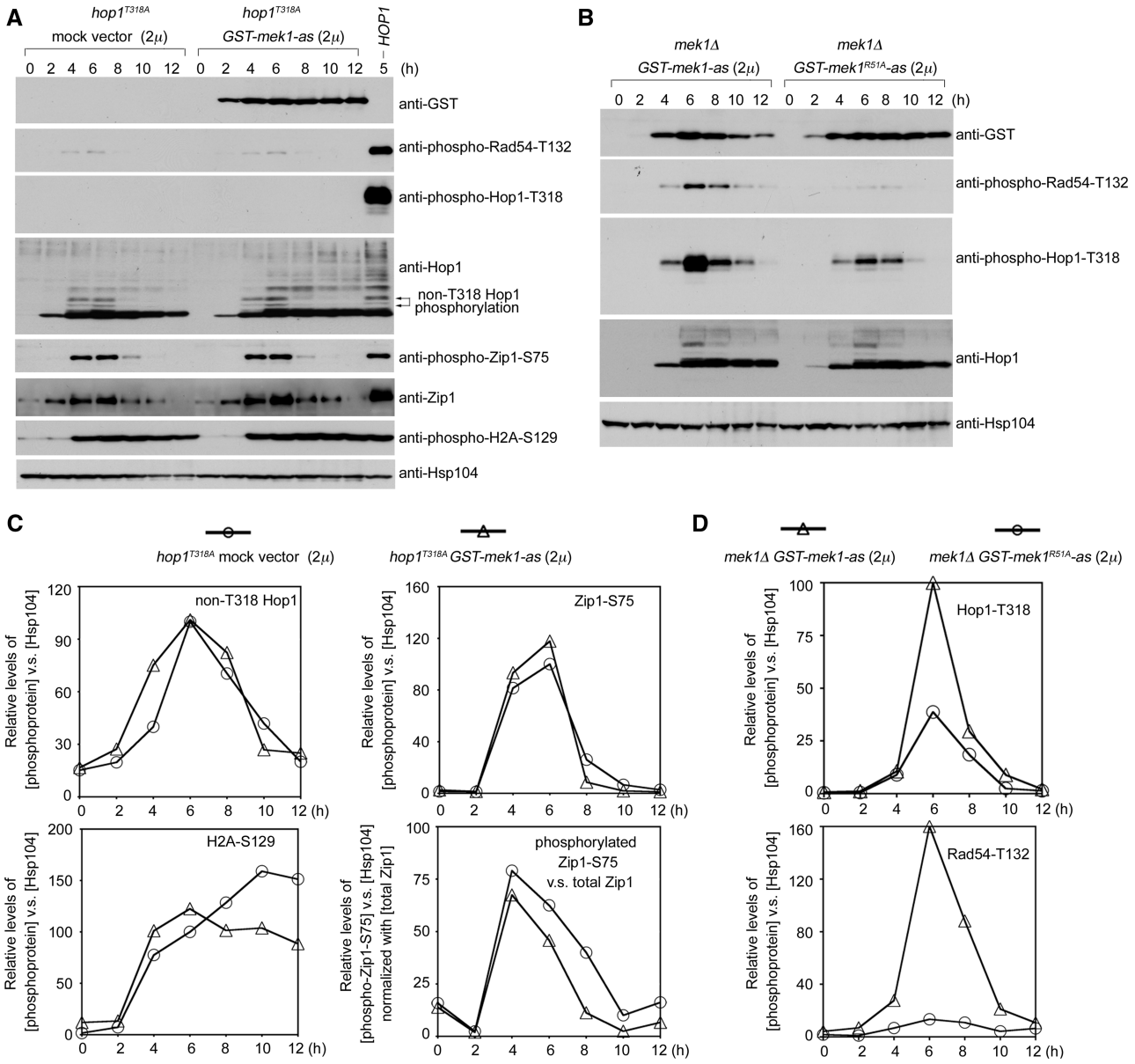

Figure 5. Hop1-T318 phosphorylation and arginine (R) 51 of Mek1 are required for the enhancement of Hop1-phosphorylation by Mek1. (**A**) *hop1*^{T318A} diploids were transformed with a mock 2 μ vector or a vector carrying *GST-MEK1-as*. (**B**) *mek1Δ* diploids were transformed with *GST-mek1-as* or *GST-mek1*^{R51A}*-as*, respectively. Western blot analyses of various phosphoproteins and proteins by the corresponding antibodies. (**C** and **D**) Quantitation of western blot results in (A) and (B).

required for the positive feedback function of Mek1 in enhancing Hop1 phosphorylation.

Arginine 51 of Mek1 is required for the enhancement of Hop1-T318 phosphorylation

Several lines of evidence suggest that Hop1 and Mek1 may act similar to the Rad53-Dun1 signaling pathway. Dun1 and Rad53 are part of the DNA damage response during *S. cerevisiae* vegetative growth. Mec1 and Tel1 first activate Rad53, which in turn activates Dun1 (56,57). These two effector kinases, similar to Mek1 (9), are characterized by the forkhead-associated (FHA) domains that are essential for their activation in response to DNA damage. Rad53 contains two SCDs (SCD1 and SCD2) with high concentrations of Mec1/Tel1 phosphorylated sites. Two threonine residues, T5 and T8, are phosphorylated in the Rad53-SCD1 (^{1}MENI^{5}T$^{[p]}$QP^{8}T$^{[p]}$QQSTQA^{15}TQRFLI^{21}E), and the diphosphorylated Rad53-SCD1 is bound by the Dun1-FHA domain (amino acid residues 19–159) to promote the phosphorylation-dependent activation of Dun1 (58,59). Two evolutionarily conserved positively charged residues (arginine 60 and lysine 100) in the Dun1-FHA domain have been shown to mediate the interaction between Dun1-FHA and diphosphorylated Rad53-SCD1 peptide (60). A structure-based sequence alignment revealed that arginine (R) 51 in Mek1-FHA is analogous to R60 in Dun1-FHA. A mutation of R51 to

alanine (A) in the Mek1-FHA domain was shown to create a null allele (*mek1*^{R51A}) (9). Notably, Rad53-SCD1 (^{5}T$^{[p]}$QP^{8}T$^{[p]}$QQST^{12}) and Hop1-SCD (^{315}IQP^{318}T$^{[p]}$QFVS^{322}) share four identical amino acid residues (QPTQ) and a phosphorylated threonine. Accordingly, Mek1-R51 and Hop1-T318 phosphorylation may act together to mediate the interaction between Mek1-FHA and the phosphorylated Hop1-SCD. Thus, we inferred that R51 of Mek1 might stabilize Hop1-T318 phosphorylation. Therefore, we examined Rad54-T132 phosphorylation and Hop1-T318 phosphorylation in *mek1Δ* diploids transformed with P_{MEK1}-*GST-mek1-as* or P_{MEK1}-*GST-mek1*^{R51A}-as. Overexpression of GST-Mek1-as or GST-Mek1^{R51A}-as did not significantly alter total Hop1 protein levels (Figure 5B, second bottom panel). We found that, unlike GST-Mek1-as, GST-Mek1^{R51A}-as promoted neither Hop1-T318 and Rad54-T132 phosphorylation (Figure 5B) nor spore viability (Table 1). These results support the model in which Mek1-FHA binds to phosphorylated Hop1-T318 and then stabilizes phosphorylated Hop1 against PP4-mediated dephosphorylation. Subsequently, Mek1 or GST-Mek1 is activated to phosphorylate Rad54-T132.

GST-Mek1 specifically enhances Hop1-T318 phosphorylation in *pch2Δ rad17Δ*

Previously, it was reported that the ectopic expression of Mek1-GST results in increased IH bias and CO formation, as well as a delayed MI phenotype, in the *pch2Δ rad17Δ* mutant (36). Rad17 is a component of the 9-1-1 checkpoint complex that promotes Mec1 kinase activity. Pch2 is a putative AAA-ATPase with important roles in pachytene checkpoint, normal SC assembly, and the distribution of DSBs and CO events (37–48). Compared with *pch2Δ*, *pch2Δ rad17Δ* exhibited lower levels of phosphorylated Rad54-T132, Hop1-T318, Zip1-S75 and H2A-S129 (Figure 6). Additionally, it has been shown that *pch2Δ rad17Δ* exhibits faster MI progression and lower spore viability than *pch2Δ* (36). We further observed markedly higher levels of Hop1-T318 phosphorylation and Rad54-T132 phosphorylation in *MEK1-GST pch2Δ rad17Δ* than in *pch2Δ rad17Δ*. Therefore, the *MEK1-GST pch2Δ rad17Δ* triple mutant is more similar to the *pch2Δ* single mutant than to the *rad17Δ pch2Δ* double mutant in terms of higher spore viability and delayed MI phenotypes (36). Consistently, the steady-state levels of phosphorylated Hop1 in *MEK1-GST pch2Δ rad17Δ* are similar to or slightly lower than those in *pch2Δ rad17Δ*, as revealed by anti-Hop1-T318 antibody and by the shifted bands detected with anti-Hop1 antibody (Figure 6). Due to a delayed MI phenotype (36), the levels of phosphorylated Rad54-T312 and Hop1-T318 persisted longer in the *MEK1-GST pch2Δ rad17Δ* triple mutant (Figure 6A). Notably, *MEK1-GST* did not significantly increase the maximum steady-state levels of H2A-S129 phosphorylation or Zip1-S75 phosphorylation in *pch2Δ rad17Δ* (Figure 4). We conclude that *MEK1-GST* did not increase the overall Mec1 and Tel1 kinase activities in *pch2Δ rad17Δ*, and that the Mek1-GST-dependent stabilization of Hop1-T318 phosphorylation is responsible for the partial rescue of the *mek1-GST pch2Δ rad17Δ* triple mutant.

DISCUSSION

The current manuscript provides new insights into the roles of the chromosome axis-associated kinase Mek1 in regulating IH recombination and checkpoint responses during yeast meiosis. Our results suggest that R51 of Mek1-FHA is critical for recognizing phosphorylated Hop1-T318 to activate Mek1 and that this interaction also stabilizes Hop1-T318 phosphorylation against PP4-dependent dephosphorylation during meiosis. The positive feedback function of Mek1 apparently does not affect Mec1 and Tel1 kinase activities on other substrates (such as Zip1-S75, H2A-S129 or non-T318 Hop1 sites). Our results also indicate that the GST-mediated dimerization may increase the protein stability of the Mek1 protein and thereby indirectly enhance Hop1-T318 phosphorylation. These findings can account for the semi-dominant phenotypes of GST-Mek1 and Mek1-GST (8,36), which rescue the spore viability of *mek1Δ* in the presence of Red1 and Hop1.

The stabilization of Hop1-T318 phosphorylation by GST-Mek1 also explains why the ectopic expression of Mek1-GST in *pch2Δ rad17Δ* promotes increased IH recombination and recombination checkpoint responses (36). The *pch2Δ rad17Δ* double mutant progresses more rapidly though MI than does the *pch2Δ* single mutant (40), and *MEK1-GST* promotes a delayed MI phenotype in *pch2Δ rad17Δ* (36). Our results indicate that the delayed MI phenotype of the *pch2Δ* single mutant and the *MEK1-GST pch2Δ rad17Δ* triple mutants are compatible with sustained elevated levels of phosphorylated Hop1-T318 and phosphorylated Rad54-T132. In contrast, less phosphorylated Hop1-T318 and phosphorylated Rad54-T132 proteins were detected in the *pch2Δ rad17Δ* double mutant, which progresses more rapidly through MI (Figure 6). Thus, the sustained elevation of Mek1 kinase activity apparently accounts for the delay in MI progression. It will be interesting to identify the downstream target(s) of Mek1 that are directly responsible for inhibiting cell cycle progression during meiotic prophase.

Our findings support a model in which Mek1 is a meiotic paralog of Dun1 in mediating cellular responses to DNA damage (Figure 7). These two checkpoint effector kinases apparently share similar upstream and downstream signaling mechanisms. The Dun1 signaling cascade involves the Mec1/Tel1-dependent phosphorylation of Rad53-SCD1. The phosphorylated Rad53-SCD1 (at T5 and T8) specifically recognizes Dun1-FHA, leading to the recruitment and activation of Dun1 to sites of DNA damage during DNA replication (56,59,60). One important function of Dun1 is the regulation of cellular dNTP levels (57,61–63). On the other hand, the Mek1 signaling cascade involves the Mec1/Tel1-dependent phosphorylation of the Hop1-SCD (21,64). The phosphorylated Hop1-SCD (T318) specifically recognizes Mek1-FHA, leading to the recruitment and activation of

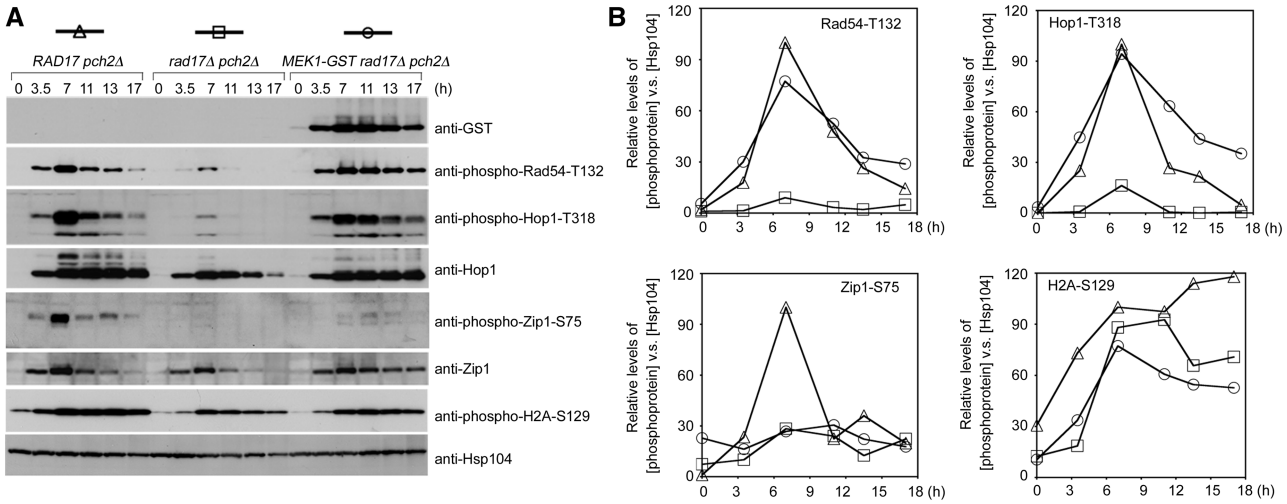

Figure 6. Mek1-GST specifically stabilizes Hop1-T318 phosphorylation in a *pch2Δ rad17Δ* mutant. Hsp104 was used as a loading control.

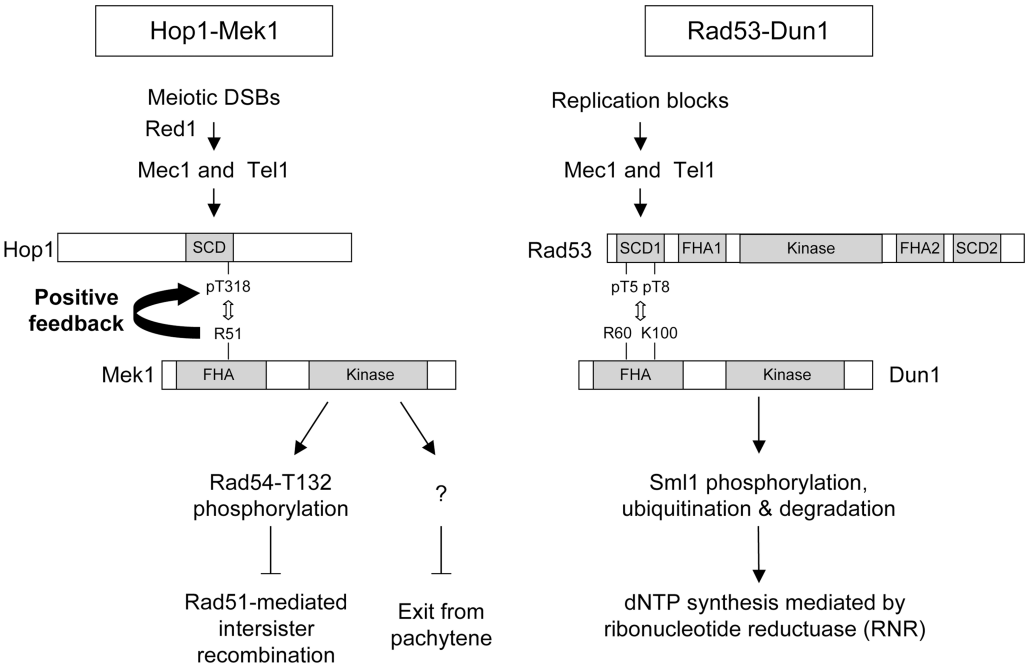

Figure 7. Mek1 is a meiotic paralog of Dun1 in mediating cellular responses to DNA damage.

Mek1 at the sites of developmentally programmed DSBs during meiotic prophase. The best-known target of Mek1 is Rad54, and Rad54 phosphorylation prevents Rad54 from binding to and activating Rad51 *in vitro* (31). Further studies will be conducted to examine whether phosphorylation-dependent inactivation (or degradation) is a general mechanism by which Mek1 regulates its downstream targets at DSB sites and chromosome axes.

ACKNOWLEDGEMENTS

The authors thank Sean Burgess (University of California, Davis), Rita Cha (MRC, London), Valentin Börner (Cleveland State University), Nancy Hollingsworth (Stony Brook University) and Douglas Bishop (University of Chicago) for the yeast strains used in this study; Chung Wang (IMB, Academia Sinica) for providing anti-Hsp104 antibodies and AndreAna Peña (IMB, Academia Sinica) for English editing.

FUNDING

Funding for open access charge: The National Science Council and Academia Sinica, Taiwan (to T.F.W.).

Conflict of interest statement. None declared.

REFERENCES

1. Keeney,S. (2001) Mechanism and control of meiotic recombination initiation. *Curr. Top. Dev. Biol.*, **52**, 1–53.
2. Kadyk,L.C. and Hartwell,L.H. (1992) Sister chromatids are preferred over homologs as substrates for recombinational repair in *Saccharomyces cerevisiae*. *Genetics*, **132**, 387–402.
3. Neale,M.J., Pan,J. and Keeney,S. (2005) Endonucleolytic processing of covalent protein-linked DNA double-strand breaks. *Nature*, **436**, 1053–1057.
4. Zakharyevich,K., Ma,Y., Tang,S., Hwang,P.Y., Boiteux,S. and Hunter,N. (2010) Temporally and biochemically distinct activities of Exo1 during meiosis: double-strand break resection and resolution of double Holliday junctions. *Mol. Cell*, **40**, 1001–1015.
5. Hodgson,A., Terentyev,Y., Johnson,R.A., Bishop-Bailey,A., Angevin,T., Croucher,A. and Goldman,A.S. (2011) Mre11 and Exo1 contribute to the initiation and processivity of resection at meiotic double-strand breaks made independently of Spo11. *DNA Repair*, **10**, 138–148.
6. San Filippo,J., Sung,P. and Klein,H. (2008) Mechanism of eukaryotic homologous recombination. *Annu. Rev. Biochem.*, **77**, 229–257.
7. Sheridan,S. and Bishop,D.K. (2006) Red-Hed regulation: recombinase Rad51, though capable of playing the leading role, may be relegated to supporting Dmc1 in budding yeast meiosis. *Genes Dev.*, **20**, 1685–1691.
8. Niu,H., Wan,L., Baumgartner,B., Schaefer,D., Loidl,J. and Hollingsworth,N.M. (2005) Partner choice during meiosis is regulated by Hop1-promoted dimerization of Mek1. *Mol. Biol. Cell*, **16**, 5804–5818.
9. Wan,L., de los Santos,T., Zhang,C., Shokat,K. and Hollingsworth,N.M. (2004) Mek1 kinase activity functions downstream of *RED1* in the regulation of meiotic double strand break repair in budding yeast. *Mol. Biol. Cell.*, **15**, 11–23.
10. Terentyev,Y., Johnson,R., Neale,M.J., Khisroon,M., Bishop-Bailey,A. and Goldman,A.S. (2010) Evidence that *MEK1* positively promotes interhomologue double-strand break repair. *Nucleic Acids Res.*, **38**, 4349–4360.
11. Goldfarb,T. and Lichten,M. (2010) Frequent and efficient use of the sister chromatid for DNA double-strand break repair during budding yeast meiosis. *PLoS Biol.*, **8**, e1000520.
12. Kim,K.P., Weiner,B.M., Zhang,L., Jordan,A., Dekker,J. and Kleckner,N. (2010) Sister cohesion and structural axis components mediate homolog bias of meiotic recombination. *Cell*, **143**, 924–937.
13. Rockmill,B. and Roeder,G.S. (1988) *RED1*: a yeast gene required for the segregation of chromosomes during the reductional division of meiosis. *Proc. Natl Acad. Sci. USA*, **85**, 6057–6061.
14. Rockmill,B. and Roeder,G.S. (1991) A meiosis-specific protein kinase homolog required for chromosome synapsis and recombination. *Genes Dev.*, **5**, 2392–2404.
15. Hollingsworth,N.M. and Ponte,L. (1997) Genetic interactions between *HOP1*, *RED1* and *MEK1* suggest that *MEK1* regulates assembly of axial element components during meiosis in the yeast *Saccharomyces cerevisiae*. *Genetics*, **147**, 33–42.
16. Smith,A.V. and Roeder,G.S. (1997) The yeast Red1 protein localizes to the cores of meiotic chromosomes. *J. Cell. Biol.*, **136**, 957–967.
17. Blat,Y., Protacio,R.U., Hunter,N. and Kleckner,N. (2002) Physical and functional interactions among basic chromosome organizational features govern early steps of meiotic chiasma formation. *Cell*, **111**, 791–802.
18. Sym,M., Engebrecht,J.A. and Roeder,G.S. (1993) Zip1 is a synaptonemal complex protein required for meiotic chromosome synapsis. *Cell*, **72**, 365–378.
19. Lin,F.M., Lai,Y.J., Shen,H.J., Cheng,Y.H. and Wang,T.F. (2010) Yeast axial-element protein, Red1, binds SUMO chains to promote meiotic interhomologue recombination and chromosome synapsis. *EMBO J.*, **29**, 586–596.
20. Eichinger,C.S. and Jentsch,S. (2010) Synaptonemal complex formation and meiotic checkpoint signaling are linked to the lateral element protein Red1. *Proc. Natl Acad. Sci. USA*, **107**, 11370–11375.
21. Carballo,J.A., Johnson,A.L., Sedgwick,S.G. and Cha,R.S. (2008) Phosphorylation of the axial element protein Hop1 by Mec1/Tel1 ensures meiotic interhomolog recombination. *Cell*, **132**, 758–770.
22. Carballo,J.A. and Cha,R.S. (2007) Meiotic roles of Mec1, a budding yeast homolog of mammalian ATR/ATM. *Chromosome Res.*, **15**, 539–550.
23. Cartagena-Lirola,H., Guerini,I., Viscardi,V., Lucchini,G. and Longhese,M.P. (2006) Budding yeast Sae2 is an in vivo target of the Mec1 and Tel1 checkpoint kinases during meiosis. *Cell Cycle*, **5**, 1549–1559.
24. Cartagena-Lirola,H., Guerini,I., Manfrini,N., Lucchini,G. and Longhese,M.P. (2008) Role of the *Saccharomyces cerevisiae* Rad53 checkpoint kinase in signaling double-strand breaks during the meiotic cell cycle. *Mol. Cell. Biol.*, **28**, 4480–4493.
25. Longhese,M.P., Bonetti,D., Guerini,I., Manfrini,N. and Clerici,M. (2009) DNA double-strand breaks in meiosis: checking their formation, processing and repair. *DNA Repair*, **8**, 1127–1138.
26. Falk,J.E., Chan,A.C., Hoffmann,E. and Hochwagen,A. (2010) A Mec1- and PP4-dependent checkpoint couples centromere pairing to meiotic recombination. *Dev. Cell*, **19**, 599–611.
27. Keogh,M.C., Kim,J.A., Downey,M., Fillingham,J., Chowdhury,D., Harrison,J.C., Onishi,M., Datta,N., Galicia,S., Emili,A. *et al.* (2006) A phosphatase complex that dephosphorylates gammaH2AX regulates DNA damage checkpoint recovery. *Nature*, **439**, 497–501.
28. O'Neill,B.M., Szyjka,S.J., Lis,E.T., Bailey,A.O., Yates,J.R. 3rd, Aparicio,O.M. and Romesberg,F.E. (2007) Pph3–Psy2 is a phosphatase complex required for Rad53 dephosphorylation and replication fork restart during recovery from DNA damage. *Proc. Natl Acad. Sci. USA*, **104**, 9290–9295.
29. Chu,S., DeRisi,J., Eisen,M., Mulholland,J., Botstein,D., Brown,P.O. and Herskowitz,I. (1998) The transcriptional program of sporulation in budding yeast. *Science*, **282**, 699–705.
30. Tung,K.S., Hong,E.J. and Roeder,G.S. (2000) The pachytene checkpoint prevents accumulation and phosphorylation of the meiosis-specific transcription factor Ndt80. *Proc. Natl Acad. Sci. USA*, **97**, 12187–12192.
31. Niu,H., Wan,L., Busygina,V., Kwon,Y., Allen,J.A., Li,X., Kunz,R.C., Kubota,K., Wang,B., Sung,P. *et al.* (2009) Regulation of meiotic recombination via Mek1-mediated Rad54 phosphorylation. *Mol. Cell*, **36**, 393–404.
32. Govin,J., Dorsey,J., Gaucher,J., Rousseaux,S., Khochbin,S. and Berger,S.L. (2010) Systematic screen reveals new functional dynamics of histones H3 and H4 during gametogenesis. *Genes Dev.*, **24**, 1772–1786.
33. Heyer,W.D., Li,X., Rolfsmeier,M. and Zhang,X.P. (2006) Rad54: the Swiss Army knife of homologous recombination? *Nucleic Acids Res.*, **34**, 4115–4125.
34. Shinohara,M., Gasior,S.L., Bishop,D.K. and Shinohara,A. (2000) Tid1/Rdh54 promotes colocalization of Rad51 and Dmc1 during meiotic recombination. *Proc. Natl Acad. Sci. USA*, **97**, 10814–10819.
35. Shinohara,M., Sakai,K., Shinohara,A. and Bishop,D.K. (2003) Crossover interference in *Saccharomyces cerevisiae* requires a *TID1*/*RDH54*- and *DMC1*-dependent pathway. *Genetics*, **163**, 1273–1286.
36. Wu,H.Y., Ho,H.C. and Burgess,S.M. (2010) Mek1 kinase governs outcomes of meiotic recombination and the checkpoint response. *Curr. Biol.*, **20**, 1707–1716.
37. San-Segundo,P.A. and Roeder,G.S. (1999) Pch2 links chromatin silencing to meiotic checkpoint control. *Cell*, **97**, 313–324.
38. San-Segundo,P.A. and Roeder,G.S. (2000) Role for the silencing protein Dot1 in meiotic checkpoint control. *Mol. Biol. Cell*, **11**, 3601–3615.
39. Bhalla,N. and Dernburg,A.F. (2005) A conserved checkpoint monitors meiotic chromosome synapsis in *Caenorhabditis elegans*. *Science*, **310**, 1683–1686.
40. Wu,H.Y. and Burgess,S.M. (2006) Two distinct surveillance mechanisms monitor meiotic chromosome metabolism in budding yeast. *Curr. Biol.*, **16**, 2473–2479.
41. Li,X.C. and Schimenti,J.C. (2007) Mouse pachytene checkpoint 2 (trip13) is required for completing meiotic recombination but not synapsis. *PLoS Genet.*, **3**, e130.

42. Borner,G.V., Barot,A. and Kleckner,N. (2008) Yeast Pch2 promotes domainal axis organization, timely recombination progression, and arrest of defective recombinosomes during meiosis. *Proc. Natl Acad. Sci. USA*, **105**, 3327–3332.
43. Joshi,N., Barot,A., Jamison,C. and Borner,G.V. (2009) Pch2 links chromosome axis remodeling at future crossover sites and crossover distribution during yeast meiosis. *PLoS Genet.*, **5**, e1000557.
44. Joyce,E.F. and McKim,K.S. (2009) Drosophila *PCH2* is required for a pachytene checkpoint that monitors double-strand-break-independent events leading to meiotic crossover formation. *Genetics*, **181**, 39–51.
45. Wojtasz,L., Daniel,K., Roig,I., Bolcun-Filas,E., Xu,H., Boonsanay,V., Eckmann,C.R., Cooke,H.J., Jasin,M., Keeney,S. *et al.* (2009) Mouse HORMAD1 and HORMAD2, two conserved meiotic chromosomal proteins, are depleted from synapsed chromosome axes with the help of TRIP13 AAA-ATPase. *PLoS Genet.*, **5**, e1000702.
46. Zanders,S. and Alani,E. (2009) The *pch2Δ* mutation in baker's yeast alters meiotic crossover levels and confers a defect in crossover interference. *PLoS Genet.*, **5**, e1000571.
47. Roig,I., Dowdle,J.A., Toth,A., de Rooij,D.G., Jasin,M. and Keeney,S. (2010) Mouse TRIP13/PCH2 is required for recombination and normal higher-order chromosome structure during meiosis. *PLoS Genet.*, **6**, e1001062.
48. Vader,G., Blitzblau,H., Tame,M., Falk,J., Curtin,L. and Hochwagen,A. (2011) Protection of repetitive DNA borders from self-induced meiotic instability. *Nature*, **477**, 115–119.
49. Ho,H.C. and Burgess,S.M. (2011) Pch2 acts through Xrs2 and Tel1/ATM to modulate interhomolog bias and checkpoint function during meiosis. *PLoS Genet.*, **7**, e1002351.
50. Redon,C., Pilch,D.R., Rogakou,E.P., Orr,A.H., Lowndes,N.F. and Bonner,W.M. (2003) Yeast histone 2A serine 129 is essential for the efficient repair of checkpoint-blind DNA damage. *EMBO Rep.*, **4**, 678–684.
51. Lai,Y.J., Lin,F.M., Chuang,M.J., Shen,H.J. and Wang,T.F. (2011) Genetic requirements and meiotic function of phosphorylation of the yeast axial element protein red1. *Mol. Cell. Biol.*, **31**, 912–923.
52. Bishop,A.C. and Shokat,K.M. (1999) Acquisition of inhibitor-sensitive protein kinases through protein design. *Pharmacol. Ther.*, **82**, 337–346.
53. Shinohara,A., Gasior,S., Ogawa,T., Kleckner,N. and Bishop,D.K. (1997) *Saccharomyces cerevisiae recA* homologues *RAD51* and *DMC1* have both distinct and overlapping roles in meiotic recombination. *Genes Cells*, **2**, 615–629.
54. Burgess,R.C., Lisby,M., Altmannova,V., Krejci,L., Sung,P. and Rothstein,R. (2009) Localization of recombination proteins and Srs2 reveals anti-recombinase function in vivo. *J. Cell. Biol.*, **185**, 969–981.
55. Xu,L., Weiner,B.M. and Kleckner,N. (1997) Meiotic cells monitor the status of the interhomolog recombination complex. *Genes Dev.*, **11**, 106–118.
56. Sanchez,Y., Zhou,Z., Huang,M., Kemp,B.E. and Elledge,S.J. (1997) Analysis of budding yeast kinases controlled by DNA damage. *Methods Enzymol.*, **283**, 398–410.
57. Chen,S.H., Smolka,M.B. and Zhou,H. (2007) Mechanism of Dun1 activation by Rad53 phosphorylation in *Saccharomyces cerevisiae*. *J. Biol. Chem.*, **282**, 986–995.
58. Bashkirov,V.I., Bashkirova,E.V., Haghnazari,E. and Heyer,W.D. (2003) Direct kinase-to-kinase signaling mediated by the FHA phosphoprotein recognition domain of the Dun1 DNA damage checkpoint kinase. *Mol. Cell. Biol.*, **23**, 1441–1452.
59. Lee,S.J., Schwartz,M.F., Duong,J.K. and Stern,D.F. (2003) Rad53 phosphorylation site clusters are important for Rad53 regulation and signaling. *Mol. Cell. Biol.*, **23**, 6300–6314.
60. Lee,H., Yuan,C., Hammet,A., Mahajan,A., Chen,E.S., Wu,M.R., Su,M.I., Heierhorst,J. and Tsai,M.D. (2008) Diphosphothreonine-specific interaction between an SQ/TQ cluster and an FHA domain in the Rad53-Dun1 kinase cascade. *Mol. Cell*, **30**, 767–778.
61. Zhao,X., Chabes,A., Domkin,V., Thelander,L. and Rothstein,R. (2001) The ribonucleotide reductase inhibitor Sml1 is a new target of the Mec1/Rad53 kinase cascade during growth and in response to DNA damage. *EMBO J.*, **20**, 3544–3553.
62. Zhao,X., Muller,E.G. and Rothstein,R. (1998) A suppressor of two essential checkpoint genes identifies a novel protein that negatively affects dNTP pools. *Mol. Cell*, **2**, 329–340.
63. Zhao,X. and Rothstein,R. (2002) The Dun1 checkpoint kinase phosphorylates and regulates the ribonucleotide reductase inhibitor Sml1. *Proc. Natl Acad. Sci. USA*, **99**, 3746–3751.
64. Niu,H., Li,X., Job,E., Park,C., Moazed,D., Gygi,S.P. and Hollingsworth,N.M. (2007) Mek1 kinase is regulated to suppress double-strand break repair between sister chromatids during budding yeast meiosis. *Mol. Cell. Biol.*, **27**, 5456–5467.